

# A Metapopulation Model for Cholera with Variable Media Efficacy and Imperfect Vaccine

Phoebe Amadi<sup>1</sup>, George Lawi<sup>2</sup> and Job Bonyo<sup>3\*</sup>

<sup>1</sup>Department of Pure and Applied Mathematics, Maseno University, P.O. Box 133- 40105, Maseno, Kenya

<sup>2</sup>Department of Mathematics, Masinde Muliro University of Science and Technology, P.O. Box 190 - 50100, Kakamega, Kenya

<sup>3</sup>Department of Mathematics, Multimedia University of Kenya, P.O. Box 15653 - 00503, Nairobi, Kenya

\*Corresponding author

## Article Info

**Keywords:** Cholera, Imperfect vaccine, Media awareness, Metapopulation, Migration

**2010 AMS:** 34C60, 34D20, 37N25

**Received:** 29 April 2023

**Accepted:** 8 November 2023

**Available online:** 25 February 2024

## Abstract

In this paper, a metapopulation model has been developed and analysed to describe the transmission dynamics of cholera between two communities linked by migration, in the presence of an imperfect vaccine and a varying media awareness impact. Stability analysis shows that the disease-free equilibrium is both locally and globally asymptotically stable when the vaccine reproduction number is less than unity. The endemic equilibria have also been shown to be locally asymptotically stable when the vaccine reproduction number is greater than unity. The simulation results show that with an imperfect vaccine and efficient media awareness, cholera transmission is reduced. The transmission rates have also been shown to be nonidentical in the two communities. It is therefore advisable, that health practitioners embrace the use of both vaccination and media awareness when designing and implementing community-specific cholera intervention strategies.

## 1. Introduction

Cholera is a diarrheal infection caused by ingestion of food or water contaminated with a gram-negative bacterium known as *Vibrio cholerae*. Humans and the aquatic environments are its main reservoirs. Majority of the infected individuals do not manifest any symptom [1]. Most of the cholera cases are presumptively diagnosed based on clinical suspicion in patients who present with severe acute watery diarrhea due to its high morbidity. If left untreated, cholera can kill within hours [1]. Its treatment depends on the severity of the illness and level of dehydration. Oral and intravenous rehydration are used to replace the lost fluids. Antibiotics are used in patients with severe volume depletion. An estimated 1.3m to 4m cholera cases with 21000 to 143000 mortalities occur annually [2, 3].

World Health Organization (WHO) recommends oral cholera vaccines as part of the integrated control program in areas at risk of cholera outbreak [4]. Two internationally-licensed oral cholera vaccines are available. Shanchol and Dukarol oral cholera vaccines have efficacies between 53% - 67% [5] and about 78% [6] respectively with Dukarol not being effective against *V. cholerae* 0139.

A multifaceted approach is key to control of cholera and to reduce related deaths. Actions targeting environmental conditions include the implementation of adapted long-term sustainable water sanitation and hygiene solutions to ensure use of safe water, basic sanitation and good hygiene practices to populations most at risk of cholera.

Cholera is more common in developing countries especially in Africa, parts of Asia and South and Central America where there is inadequate access to safe drinking water and poor sanitation facilities. In the 21<sup>st</sup> C, Sub-Saharan Africa bears the brunt of global cholera [7] where the countries face the dual challenges of improving both cholera treatment and access to basic health care, prevention and improved water and sanitation systems.

In Kenya, cholera is endemic in many parts of the country with sporadic outbreaks especially during rainy seasons and in informal settlements. Currently there has been cholera outbreaks in Wajir, Mandera, Machakos, Garissa, Migori and Kisumu counties. Evidently, socio-economic differences between regions would determine the efficacy of some strategies especially those targeting sanitation and hygiene.

A number of mathematical models have been developed to analyze the disease transmission dynamics. The dynamics and optimal control

strategies for cholera epidemics was developed and analysed in [8] under the interventions; vaccination, treatment and education awareness. The analysis indicates that vaccination and education campaigns should be applied from the start of an outbreak followed by treatment. However, the effects of vaccination and education campaigns could be affected by migration of especially the asymptotically infected individuals.

The impact of media coverage on the spread of cholera was investigated in [9]. The numerical analysis shows that the disease dies out faster in the presence of media coverage. It's noteworthy that a combination of preventive and therapeutic strategies is likely to lead to a better outcome. A metapopulation model for cholera dynamics between two communities, in the presence of controls was developed and analysed in [10]. A model investigating the influence of cultural practices on the dynamics of cholera is presented in [3]. Modeling optimal intervention strategies for cholera is presented in [11]. A cost-effective balance of multiple intervention methods is compared for two endemic populations. The impact of spatial arrangements on epidemic disease dynamics and intervention strategies for cholera is investigated in [12]. The effects of vaccination, water chlorination and proper hygiene is investigated. The analysis shows that the infection may be eight times less devastating in the presence of controls. This model assumes uniform efficacy of the control strategies in the communities involved, and that vaccinated individuals are fully protected against the infection. These assumptions may not be entirely realistic since cholera vaccines are not 100% efficacious and the socio-economic differences between communities connected via migration is likely to determine the efficacy of control strategies. This work is largely part of the thesis [13].

### 1.1. Mathematical approaches in analyzing cholera transmission dynamics

A stochastic mathematical model with the rate of contact with the environment and the untreated individuals rate of recovery being subjected to some random interference was developed in [14]. The model investigates the behavior of solutions of a stochastic cholera model near the disease-free equilibrium and its corresponding deterministic endemic equilibrium. A mathematical model based on the general form of the Caputo fractional derivative is investigated for a real-world cholera outbreak in [2].

Mehmet et al [15] incorporated the random effects to the parameters of a deterministic model for the transmission dynamics of cholera to study the change of findings for Laplacian and Triangular distributions. Using Fuzzy set theory, [16] developed a cholera model in which all of the parameters were fuzzy numbers. The model study reveals that the imprecise parameter values have had a significant impact on both human and bacterial populations. In this paper, the dynamics of cholera transmission in two communities connected via migration when vaccination and media awareness are at different efficacy levels is explored.

## 2. Model Formulation and Description

To develop the metapopulation model, the general population considered is divided into two main communities and each community divided into four compartments with reference to vaccination of the susceptible individuals, impact of media awareness, *Vibrios* transmission and the disease states of the individuals. This model assumes that each community is homogeneous in the sense that there are no socio-economic barriers to interaction and a special heterogeneity which is accounted for by the immigrations. The compartments involve individuals who are susceptible ( $S_i$ ), the susceptible individuals who have been vaccinated against cholera ( $V_i$ ), those infected symptomatically and asymptotically ( $I_i$ ) and those individuals who have recovered ( $R_i$ ) from the infection. The total population  $N_i$ , ( $i = 1, 2$ ), of this model is given by;

$$N_i = S_i + V_i + I_i + R_i.$$

This model accounts for movement of asymptotically infected individuals from one community to another. This group plays a vital role in metapopulation transmission modeling of cholera since they contribute to the disease transmission for a relatively long time. The role played by the asymptotically infected individuals range from person to person transmission as well as shedding of the pathogens into the aquatic reservoirs. The symptomatically infected individuals are assumed to be quarantined in hospitals for treatment as soon as they are identified. The recruitment of the susceptible individuals into the communities are at the rates  $\Lambda_1$  and  $\Lambda_2$  for the first and the second communities respectively. This intrinsic difference rate is mainly the difference of births, deaths and immigrations at the time of modeling. Vaccination of the susceptible individuals is at the rates  $\omega_1$  and  $\omega_2$  for the first and second communities respectively, with  $0 < \sigma_i < 1$ , for  $i = 1, 2$  denoting the vaccine efficacy. This implies that when  $\sigma$  is close to one, the vaccine is very effective and the disease transmission is low and when  $\sigma$  is close to zero, the vaccine is not effective and the disease transmission is high. Considering the relatively long vaccine protection period [1], this model excludes vaccinated individuals whose immunity has waned off to become susceptible.

The concentration of *Vibrios* in the environment is denoted by  $B_1$  and  $B_2$  for the first and second communities respectively. The susceptible individuals acquire cholera infection through ingestion of environmental *Vibrios* from contaminated water reservoirs at the rates  $\lambda_{ei}$  and through human-to-human transmission after ingestion of hyperinfectious *Vibrios* at the rates  $\lambda_{hi}$  for  $i = 1, 2$ , where;

$$\lambda_{ei} = (1 - \rho_i) \frac{\beta_{ei} B_i}{k + B_i}, \text{ and } \lambda_{hi} = (1 - \rho_i) \frac{\beta_{hi} I_i}{m + I_i}.$$

The susceptible population is infected following ingestion of *Vibrios* from aquatic reservoirs at the rate  $\beta_{ei}$  and  $(1 - \rho_i)\beta_{ei}$ , is the reduced rate of ingestion of *Vibrios* from the environment due to media awareness, where  $0 < \rho_i < 1$  measures the efficacy of media awareness. The half saturation constant of the pathogen population, enough to make an individual to contract the infection is denoted by  $k > 0$ . The saturation incidence function  $\frac{\beta_{ei} B_i}{k + B_i}$  ensures boundedness of the incidence rate of infection from the environment and indicates that the incidence rate is gradual rather than linear.  $\beta_{hi}$  is the effective contact rate for human-to-human transmission. The minimum contact rate with an infected person that can cause about 50% chance of contracting the infection is denoted by  $m$ .  $\frac{I_i}{m + I_i}$  is a continuous bounded function which takes into account the disease saturation.

The natural death rates in the first and second communities are denoted by  $\mu_1$  and  $\mu_2$  respectively. The infected individuals recover from the infection at the rates  $\gamma_1$  and  $\gamma_2$  and suffer disease induced mortality at the rates  $\delta_1$  and  $\delta_2$  for the first and second communities respectively. The recovered individuals are assumed to develop some immunity after recovery, and cannot be infected again in one outbreak [17]. The movement of asymptotically infected individuals across the communities is at the rates  $a_1$  and  $a_2$  for the first and second communities

respectively. Infected individuals shed bacteria into the environment at the rates  $\xi_1$  and  $\xi_2$  in the first and second communities respectively. The decay rates of the pathogens is denoted by  $\mu_{1p}$  and  $\mu_{2p}$  while the multiplication rates of pathogens in the aquatic reservoirs is denoted by  $g_1$  and  $g_2$  in the first and second communities respectively. The above description is captured in the flow chart diagram in Figure 2.1. A mathematical equivalent is given in terms of system of ordinary differential equations (2.1).

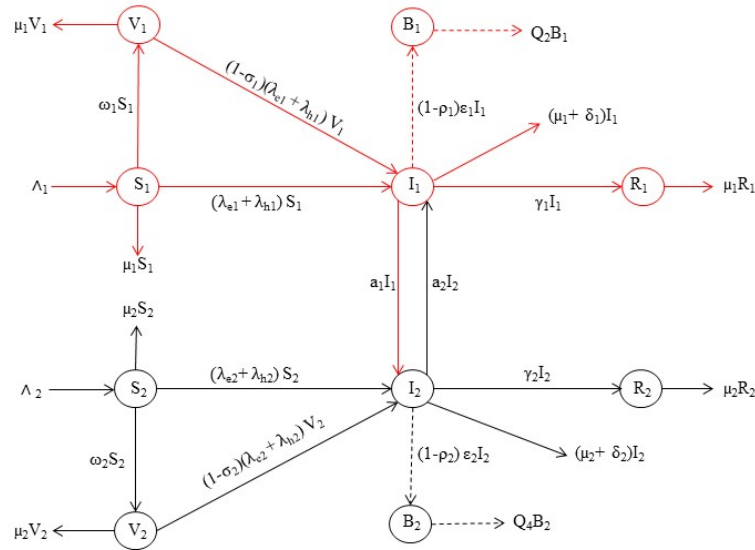


**Figure 2.1:** The Flow Diagram for the Metapopulation Model.

$$\begin{aligned}
 \frac{dS_1}{dt} &= \Lambda_1 - \omega_1 S_1 - [\lambda_{e1} + \lambda_{h1}] S_1 - \mu_1 S_1 \\
 \frac{dV_1}{dt} &= \omega_1 S_1 - (1 - \sigma_1) [\lambda_{e1} + \lambda_{h1}] V_1 - \mu_1 V_1 \\
 \frac{dI_1}{dt} &= [\lambda_{e1} + \lambda_{h1}] S_1 + (1 - \sigma_1) [\lambda_{e1} + \lambda_{h1}] V_1 + a_2 I_2 - Q_1 I_1 \\
 \frac{dR_1}{dt} &= \gamma_1 I_1 - \mu_1 R_1 \\
 \frac{dB_1}{dt} &= (1 - \rho_1) \xi_1 I_1 - Q_2 B_1 \\
 \frac{dS_2}{dt} &= \Lambda_2 - \omega_2 S_2 - [\lambda_{e2} + \lambda_{h2}] S_2 - \mu_2 S_2 \\
 \frac{dV_2}{dt} &= \omega_2 S_2 - (1 - \sigma_2) [\lambda_{e2} + \lambda_{h2}] V_2 - \mu_2 V_2 \\
 \frac{dI_2}{dt} &= [\lambda_{e2} + \lambda_{h2}] S_2 + (1 - \sigma_2) [\lambda_{e2} + \lambda_{h2}] V_2 + a_1 I_1 - Q_3 I_2 \\
 \frac{dR_2}{dt} &= \gamma_2 I_2 - \mu_2 R_2 \\
 \frac{dB_2}{dt} &= (1 - \rho_2) \xi_2 I_2 - Q_4 B_2,
 \end{aligned}$$

where  $Q_1 = \mu_1 + \delta_1 + \gamma_1 + a_1$ ,  $Q_2 = \mu_{1p} - g_1$ ,  $Q_3 = \mu_2 + \delta_2 + \gamma_2 + a_2$ ,  $Q_4 = \mu_{2p} - g_2$ .  $Q_2$  and  $Q_4$  are positive such that in the presence of improved hygiene and sanitation and reduced shedding rate of the pathogens by the infected individuals, the bacteria cannot sustain themselves in the aquatic environment [18]. The equation for the recovered compartment is decoupled in equation (2.1), thus it is enough to

consider the following reduced system of equations:

$$\begin{aligned}
 \frac{dS_1}{dt} &= \Lambda_1 - \omega_1 S_1 - [\lambda_{e1} + \lambda_{h1}] S_1 - \mu_1 S_1 \\
 \frac{dV_1}{dt} &= \omega_1 S_1 - (1 - \sigma_1) [\lambda_{e1} + \lambda_{h1}] V_1 - \mu_1 V_1 \\
 \frac{dI_1}{dt} &= [\lambda_{e1} + \lambda_{h1}] S_1 + (1 - \sigma_1) [\lambda_{e1} + \lambda_{h1}] V_1 + a_2 I_2 - Q_1 I_1 \\
 \frac{dB_1}{dt} &= (1 - \rho_1) \xi_1 I_1 - Q_2 B_1 \\
 \frac{dS_2}{dt} &= \Lambda_2 - \omega_2 S_2 - [\lambda_{e2} + \lambda_{h2}] S_2 - \mu_2 S_2 \\
 \frac{dV_2}{dt} &= \omega_2 S_2 - (1 - \sigma_2) [\lambda_{e2} + \lambda_{h2}] V_2 - \mu_2 V_2 \\
 \frac{dI_2}{dt} &= [\lambda_{e2} + \lambda_{h2}] S_2 + (1 - \sigma_2) [\lambda_{e2} + \lambda_{h2}] V_2 + a_1 I_1 - Q_3 I_2 \\
 \frac{dB_2}{dt} &= (1 - \rho_2) \xi_2 I_2 - Q_4 B_2.
 \end{aligned}
 \tag{2.1}$$

### 3. Model Analysis and Discussion

#### 3.1. Positivity and boundedness of solutions

##### 3.1.1. Positivity of solutions

The well posedness of the model is established by showing that its solutions are positive and bounded. An assumption is made that the initial conditions of system (2.1) are non-negative since the model monitors populations. Therefore,  $S_i(0) > 0, V_i(0) \geq 0, I_i(0) \geq 0, B_i(0) \geq 0$  for  $i = 1, 2$ . The total population for each community satisfies  $\frac{dN_i(t)}{dt} = \Lambda_i - \mu_i N_i - \delta_i$  and the total population size for the two communities is  $N(t) = \sum_{i=1}^2 (N_i(t))$ .

**Theorem 3.1.** *Let the initial conditions be  $S_i(0) > 0, V_i(0) \geq 0, I_i(0) \geq 0, B_i(0) \geq 0$ , then the solution set  $\{S_i(t), V_i(t), I_i(t), B_i(t)\}$  ( $i = 1, 2$ ) of the model system (2.1) is positive for all  $t > 0$ .*

*Proof.* From the first equation of system (2.1);

$$\frac{dS_i}{dt} = \Lambda_i - \omega_i S_i - \lambda_{ei} S_i - \lambda_{hi} S_i - \mu_i S_i,$$

implying that

$$\frac{dS_i}{dt} \geq -[\omega_i + \lambda_{ei} + \lambda_{hi} + \mu_i] S_i.$$

Integration yields

$$S_i(t) \geq e^{-[\omega_i + \lambda_{ei} + \lambda_{hi} + \mu_i]t} e^C$$

for some constant C. Hence,  $S_i(t) > 0$  for all  $t \geq 0$ . Similarly, it can also be shown that the other solutions are non-negative for all  $t \geq 0$ .  $\square$

##### 3.1.2. Boundedness of the solutions

The model solutions are shown to be bounded in the invariant region  $\Omega$  where  $\Omega = \{(S_1, V_1, I_1, B_1, S_2, V_2, I_2, B_2) : N_i \leq \frac{\Lambda_i}{\mu_i}\}$  for  $i = 1, 2$ .

**Theorem 3.2.** *The solutions of the model system (2.1) are bounded in the feasible region  $\Omega$ .*

*Proof.* Since the initial conditions for system (2.1) are non-negative,  $\Omega = \bigcup_{i=1}^2 \Omega_i$  and that each community is a closed community with respect to the adjacent community, the time derivative of  $N_i(t)$  for ( $i = 1, 2$ ) is given by

$$\frac{dN_i}{dt} = \Lambda_i - \mu_i (S_i + V_i + I_i + R_i) - \delta_i I_i,$$

and therefore

$$\frac{dN_i}{dt} + \mu_i N_i \leq \Lambda_i.$$

By solving, we obtain  $N_i(t) \leq \frac{\Lambda_i}{\mu_i} + e^{-\mu_i t} C$  for some positive constant C.

Thus  $N_i(0) \leq \frac{\Lambda_i}{\mu_i} + C$  and  $\lim_{t \rightarrow \infty} N_i(t) \leq \frac{\Lambda_i}{\mu_i} + C$ . Hence  $0 < N_i(t) \leq \frac{\Lambda_i}{\mu_i} + C$  ( $i = 1, 2$ ) for all  $t \geq 0$ , which implies that the solutions of system (2.1) are bounded in the invariant region  $\Omega$ . Thus the model is mathematically well posed and biologically meaningful in the feasible region  $\Omega$ .  $\square$

### 3.2. Stability analysis

An equilibrium point is defined as a steady state solution of a model. The stability of model (2.1) is analysed in order determine the impact of imperfect vaccine and variable media awareness on the epidemiology of cholera between the two communities linked via migration. The existence of the equilibrium points of model (2.1) with respect to the basic reproduction number is derived using the next generation matrix approach.

#### 3.2.1. Disease free equilibrium ( $E_0$ )

The disease free equilibrium (DFE) is a steady state solution of a mode. It is obtained by setting the right hand side of equation (2.1) to zero and solving with  $I_i = B_i = 0$  ( $i = 1, 2$ ). This yields  $E_0 = (S_1, V_1, 0, 0, S_2, V_2, 0, 0) \in \mathbb{R}_+^8$  which is equal to

$$E_0 = \left[ \frac{\Lambda_1}{\mu_1 + \omega_1}, \frac{\Lambda_1 \omega_1}{\mu_1(\mu_1 + \omega_1)}, 0, 0, \frac{\Lambda_2}{\mu_2 + \omega_2}, \frac{\Lambda_2 \omega_2}{\mu_2(\mu_2 + \omega_2)}, 0, 0 \right] \tag{3.1}$$

Suppose there is no infection in a given population such that there is no infective, the solution of the systems of equations (2.1) corresponding to this state is the disease free equilibrium given by equation (3.1). This provides a baseline for analyzing the long term dynamics of cholera infection in the two communities under study.

#### 3.2.2. Basic and vaccine reproduction numbers

Basic reproduction number  $R_0$  is the average number of secondary infections caused by a single infected agent during his/her entire infectious period, in a completely susceptible population. It sets the threshold in the study of a disease both for predicting its outbreak and for evaluating its control strategies. Theoretically, if  $R_0 < 1$ , then every infectious individual will cause less than one secondary infection and hence the disease will die out and when  $R_0 > 1$ , then every infectious individual will cause more than one secondary infection, hence the disease will be persistent in the population. A larger value of  $R_0$  may indicate the possibility of a major epidemic. The vaccine reproduction number for model (2.1) is determined using the next generation matrix approach by Driessche et al [19] as:

$$R_{V1} = \frac{(\mu_1 + \eta_1 \omega_1)(\alpha_1 \beta_{h1} \Lambda_1 k Q_2 + \alpha_1^2 \beta_{e1} \Lambda_1 \xi_1 m)}{\mu_1(\mu_1 + \omega_1)kQ_1Q_2m} \tag{3.2}$$

and

$$R_{V2} = \frac{(\mu_2 + \eta_2 \omega_2)(\alpha_2 \beta_{h2} \Lambda_2 k Q_4 + \alpha_2^2 \beta_{e2} \Lambda_2 \xi_2 m)}{\mu_2(\mu_2 + \omega_2)kQ_3Q_4m},$$

where  $R_{V1}$  and  $R_{V2}$  are the vaccine reproduction numbers for community one and two respectively with  $\alpha_i = 1 - \rho_i$  and  $\eta_i = 1 - \sigma_i$ , ( $i = 1, 2$ ). In the absence of the intervention strategies (vaccination and media awareness) and the parameters  $\omega_i$  and  $\rho_i$ ,  $i = 1, 2$  are set to zero, then the basic reproduction numbers for the two communities are determined as:

$$R_{01} = \frac{\beta_{h1} \Lambda_1 k Q_2 + \beta_{e1} \Lambda_1 \xi_1 m}{\mu_1 k Q_1 Q_2 m} \tag{3.3}$$

and

$$R_{02} = \frac{\beta_{h2} \Lambda_2 k Q_4 + \beta_{e2} \Lambda_2 \xi_2 m}{\mu_2 k Q_3 Q_4 m},$$

where  $R_{01}$  and  $R_{02}$  are the basic reproduction numbers for community one and two respectively. This basic reproduction number is used to analyze the stability of the equilibrium points of model (2.1).

#### 3.2.3. Local stability of the disease free equilibrium

To investigate the local stability of the disease free equilibrium ( $E_0$ ), the method described in [19] is employed to linearize the model system (2.1).

**Theorem 3.3.** *The disease free equilibrium ( $E_0$ ) is locally asymptotically stable if  $R_{Vi} < 1$  ( $i = 1, 2$ ) and unstable otherwise.*

*Proof.* The Jacobian matrix of system (2.1) evaluated at  $E_0$  is given by;

$$J(E_0) = \begin{bmatrix} -(\omega_1 + \mu_1) & 0 & -\frac{\alpha_1 \beta_{h1} \Lambda_1}{(\mu_1 + \omega_1)m} & -\frac{\alpha_1 \beta_{e1} \Lambda_1}{(\mu_1 + \omega_1)k} \\ \omega_1 & -\mu_1 & -\frac{\eta_1 \alpha_1 \beta_{h1} \Lambda_1 \omega_1}{\mu_1(\mu_1 + \omega_1)m} & -\frac{\eta_1 \alpha_1 \beta_{e1} \Lambda_1 \omega_1}{\mu_1(\mu_1 + \omega_1)k} \\ 0 & 0 & \frac{(\mu_1 + \eta_1 \omega_1) \alpha_1 \beta_{h1} \Lambda_1}{\mu_1(\mu_1 + \omega_1)m} - Q_1 & \frac{(\mu_1 + \eta_1 \omega_1) \alpha_1 \beta_{e1} \Lambda_1}{\mu_1(\mu_1 + \omega_1)k} \\ 0 & 0 & \alpha_1 \xi_1 & -Q_2. \end{bmatrix}$$

An equilibrium point is locally asymptotically stable if its Jacobian matrix has a negative trace and a positive determinant or if all its eigenvalues have negative real parts [20]. The Jacobian matrix  $J(E_0)$  has two distinct negative eigenvalues given by  $-\mu_1$  and  $-(\omega_1 + \mu_1)$ . The local stability of  $E_0$  is studied by examining the trace and determinant of the reduced block matrix  $J(E_0^*)$  defined by;

$$J(E_0^*) = \begin{bmatrix} \frac{(\mu_1 + \eta_1 \omega_1) \alpha_1 \beta_{h1} \Lambda_1}{\mu_1 (\mu_1 + \omega_1) m} - Q_1 & \frac{(\mu_1 + \eta_1 \omega_1) \alpha_1 \beta_{e1} \Lambda_1}{\mu_1 (\mu_1 + \omega_1) k} \\ \alpha_1 \xi_1 & -Q_2 \end{bmatrix}.$$

Using the conditions outlined in [9], let  $Tr$  be the Trace and  $Det$  be the Determinant of the block matrix  $J(E_0^*)$ . For the eigenvalues of  $J(E_0^*)$  to be negative, then  $Det(J(E_0^*)) > 0$  and  $Tr(J(E_0^*)) < 0$ . The conditions that will make this to hold are thus determined.

For  $Det(J(E_0^*)) > 0$ , then;

$$\frac{(\mu_1 + \eta_1 \omega_1) (\alpha_1 \beta_{h1} \Lambda_1 k Q_2 + \alpha_1^2 \beta_{e1} \Lambda_1 \xi_1 m)}{\mu_1 (\mu_1 + \omega_1) km} < Q_1 Q_2. \tag{3.4}$$

Simplifying inequality (3.4) yields;

$$\frac{(\mu_1 + \eta_1 \omega_1) (\alpha_1 \beta_{h1} \Lambda_1 k Q_2 + \alpha_1^2 \beta_{e1} \Lambda_1 \xi_1 m)}{\mu_1 (\mu_1 + \omega_1) k Q_1 Q_2 m} < 1. \tag{3.5}$$

Since the LHS of inequality (3.5) equals to  $R_{V1}$ , the determinant of  $J(E_0^*)$  can only be positive if  $R_{V1} < 1$ .

For  $Tr(J(E_0^*)) < 0$ , then;

$$\frac{\alpha_1 \beta_{h1} \Lambda_1 (\mu_1 + \eta_1 \omega_1)}{\mu_1 (\mu_1 + \omega_1) m} - Q_1 < 0. \tag{3.6}$$

Making  $Q_1$  the subject of equation (3.2), yields;

$$Q_1 = \frac{(\mu_1 + \eta_1 \omega_1) (\alpha_1 \beta_{h1} \Lambda_1 k Q_2 + \alpha_1^2 \beta_{e1} \Lambda_1 \xi_1 m)}{\mu_1 (\mu_1 + \omega_1) k Q_2 m R_{V1}}. \tag{3.7}$$

Substituting equation (3.7) into inequality (3.6) gives;

$$\frac{\alpha_1 \beta_{h1} \Lambda_1 (\mu_1 + \eta_1 \omega_1)}{\mu_1 (\mu_1 + \omega_1) m} - \frac{(\mu_1 + \eta_1 \omega_1) (\alpha_1 \beta_{h1} \Lambda_1 k Q_2 + \alpha_1^2 \beta_{e1} \Lambda_1 \xi_1 m)}{\mu_1 (\mu_1 + \omega_1) k Q_2 m R_{V1}} < 0. \tag{3.8}$$

Simplifying inequality (3.8) yields;

$$\frac{\phi_1 \alpha_1 \Lambda_1}{\mu_1 (\mu_1 + \omega_1) m} \left[ \beta_{h1} \left( 1 - \frac{1}{R_{V1}} \right) - \frac{\alpha_1 \beta_{e1} \xi_1 m}{k Q_2 R_{V1}} \right] < 0,$$

which can only hold if  $R_{V1} < 1$ , implying that the  $Tr(J(E_0^*)) < 0$  if  $R_{V1} < 1$ . Hence, the disease free equilibrium is locally asymptotically stable if  $R_{V1} < 1$ . Similarly, it can also be shown that the disease free equilibrium of the second community is also locally asymptotically stable when  $R_{V2} < 1$ .  $\square$

### 3.2.4. Global stability of the disease free equilibrium

To investigate the global stability of the disease free equilibrium, Castillo-Chavez theorem [21] is employed. System (2.1) is rewritten in the form;

$$\begin{aligned} \frac{dX}{dt} &= F(X, Z) \\ \frac{dZ}{dt} &= G(X, Z), G(X, 0) = 0, \end{aligned} \tag{3.9}$$

where  $X = (S_1, V_1, S_2, V_2)$ ,  $X \in \mathbb{R}^4$  denotes (its components) the uninfected individuals while  $Z = (I_1, B_1, I_2, B_2)$ ,  $Z \in \mathbb{R}^4$  denotes (its components) the infected individuals.  $E_0 = (X^*, 0)$  is the disease free equilibrium of system (3.9). According to [21], the following conditions (H1) and (H2) must be met to guarantee local asymptotic stability of the system:

(H1) For  $\frac{dX}{dt} = F(X, 0)$ ,  $X^*$  is globally asymptotically stable (g.a.s),

(H2)  $G(X, Z) = AZ - \widehat{G}(X, Z)$ ,  $\widehat{G}(X, Z) \geq 0$  for  $(X, Z) \in \Omega$ ,

where  $A = D_Z G(X^*, 0)$  is a Metzler Matrix (the off diagonal elements are nonnegative) and  $\Omega$  is the region where the model makes biological sense. Castillo-Chavez theorem provides that  $E_0$  will be globally asymptotically stable if it's locally asymptotically stable and satisfies (H1) and (H2).

**Theorem 3.4.** *The disease free equilibrium ( $E_0$ ) is locally asymptotically stable whenever  $R_{Vi} < 1$  ( $i = 1, 2$ ).*

*Proof.* Using the above notation, we have

$$\frac{dX}{dt} = \begin{bmatrix} \frac{dS_1}{dt} = \Lambda_1 - (\omega_1 + \mu_1) S_1 \\ \frac{dV_1}{dt} = \omega_1 S_1 - \mu_1 V_1 \\ \frac{dS_2}{dt} = \Lambda_2 - (\omega_2 + \mu_2) S_2 \\ \frac{dV_2}{dt} = \omega_2 S_2 - \mu_2 V_2 \end{bmatrix}$$

and solving for  $S_1, V_1, S_2, V_2$  yields  $S_1(t) = \frac{\Lambda_1}{\omega_1 + \mu_1} + Ce^{-(\omega_1 + \mu_1)t}$ ;  $V_1(t) = \frac{\omega_1 \Lambda_1}{\mu_1(\omega_1 + \mu_1)} + Ce^{-(\mu_1)t}$ ,  $S_2 = \frac{\Lambda_2}{\omega_2 + \mu_2} + Ce^{-(\omega_2 + \mu_2)t}$  and  $V_2(t) = \frac{\omega_2 \Lambda_2}{\mu_2(\omega_2 + \mu_2)} + Ce^{-(\mu_2)t}$ . Therefore  $\lim_{t \rightarrow \infty} X(t) = \left[ \frac{\Lambda_1}{\mu_1 + \omega_1}, \frac{\omega_1 \Lambda_1}{\mu_1(\mu_1 + \omega_1)}, \frac{\Lambda_2}{\mu_2 + \omega_2}, \frac{\omega_2 \Lambda_2}{\mu_2(\mu_2 + \omega_2)} \right] = X^*$ , implying that  $X^*$  is globally asymptotically stable. Hence, condition (H1) is satisfied.

Now, the matrix  $A$  is determined as:

$$A = \begin{bmatrix} \frac{\alpha_1 \beta_{h1} d_1}{m} - Q_1 & \frac{\alpha_1 \beta_{e1} d_1}{k} & a_2 & 0 \\ \alpha_1 \xi_1 & -Q_2 & 0 & 0 \\ a_1 & 0 & \frac{\alpha_2 \beta_{h2} d_2}{m} - Q_3 & \frac{\alpha_2 \beta_{e2} d_2}{k} \\ 0 & 0 & \alpha_2 \xi_2 & -Q_4 \end{bmatrix}$$

where  $d_1 = S_1 + \eta_1 V_1$  and  $d_2 = S_2 + \eta_2 V_2$ ;

$$AZ = \begin{bmatrix} \frac{\alpha_1 \beta_{h1} d_1 I_1}{m} - Q_1 I_1 + \frac{\alpha_1 \beta_{e1} d_1 B_1}{k} + a_{21} I_2 \\ \alpha_1 \xi_1 I_1 - Q_2 B_1 \\ a_{12} I_1 + \frac{\alpha_2 \beta_{h2} d_2 I_2}{m} - Q_3 I_2 + \frac{\alpha_2 \beta_{e2} d_2 B_2}{k} \\ \alpha_2 \xi_2 I_2 - Q_4 B_2 \end{bmatrix},$$

$$G(X, Z) = \begin{bmatrix} \left( \frac{\alpha_1 \beta_{e1} B_1}{k+B_1} + \frac{\alpha_1 \beta_{h1} I_1}{m+I_1} \right) S_1 + \eta_1 \left( \frac{\alpha_1 \beta_{e1} B_1}{k+B_1} + \frac{\alpha_1 \beta_{h1} I_1}{m+I_1} \right) V_1 + a_{21} I_2 - Q_1 I_1 \\ \alpha_1 \xi_1 I_1 - Q_2 B_1 \\ \left( \frac{\alpha_2 \beta_{e2} B_2}{k+B_2} + \frac{\alpha_2 \beta_{h2} I_2}{m+I_2} \right) S_2 + \eta_2 \left( \frac{\alpha_2 \beta_{e2} B_2}{k+B_2} + \frac{\alpha_2 \beta_{h2} I_2}{m+I_2} \right) V_2 + a_{12} I_1 - Q_3 I_2 \\ \alpha_2 \xi_2 I_2 - Q_4 B_2 \end{bmatrix},$$

and

$$\widehat{G}(X, Z) = \begin{bmatrix} \frac{\alpha_1 \beta_{h1} I_1^2 S_1}{m(m+I_1)} + \frac{\eta_1 \alpha_1 \beta_{h1} I_1^2 V_1}{m(m+I_1)} + \frac{\alpha_1 \beta_{e1} B_1^2 S_1}{k(k+B_1)} + \frac{\eta_1 \alpha_1 \beta_{e1} B_1^2 V_1}{k(k+B_1)} \\ 0 \\ \frac{\alpha_2 \beta_{h2} I_2^2 S_2}{m(m+I_2)} + \frac{\eta_2 \alpha_2 \beta_{h2} I_2^2 V_2}{m(m+I_2)} + \frac{\alpha_2 \beta_{e2} B_2^2 S_2}{k(k+B_2)} + \frac{\eta_2 \alpha_2 \beta_{e2} B_2^2 V_2}{k(k+B_2)} \\ 0 \end{bmatrix}.$$

Therefore  $\widehat{G}(X, Z) = AZ - G(X, Z) \geq 0$  as all the parameters used are positive and  $0 < \alpha_i, \eta_i < 1$  for  $i = 1, 2$ ; implying that the condition (H2) has been met as well. Since  $E_0$  is locally asymptotically stable if  $R_{V_i} < 1$  ( $i = 1, 2$ ) and the conditions (H1) and (H2) are satisfied, it follows from Castillo-Chavez theorem that  $E_0$  is globally asymptotically stable equilibrium of model (2.1) whenever  $R_{V_i} < 1$ .  $\square$

### 3.2.5. Boundary endemic steady state

The model has boundary endemic equilibrium point when the infection is persistent in one community but is absent in the other. The boundary endemic equilibrium points are obtained by setting the equations of system (2.1) to zero. Note that at the first boundary endemic equilibrium point  $E_1 = (S_1^*, V_1^*, I_1^*, B_1^*, S_2, V_2, 0, 0)$ , the disease is persistent only in the first community and at the second boundary endemic equilibrium point  $E_2 = (S_1, V_1, 0, 0, S_2^*, V_2^*, I_2^*, B_2^*)$ , the disease is persistent only in the second community.

**Theorem 3.5.** *The first boundary endemic equilibrium point ( $E_1$ ) exists provided that  $R_{V_1} > 1$ .*

*Proof.* For the existence of the first boundary endemic equilibrium, the equations of system (2.1) at  $E_1$  becomes;

$$\begin{aligned} 0 &= \Lambda_1 - \omega_1 S_1 - \lambda_{e1} S_1 - \lambda_{h1} S_1 - \mu_1 S_1 \\ 0 &= \omega_1 S_1 - \eta_1 [\lambda_{e1} V_1 + \lambda_{h1} V_1] - \mu_1 V_1 \\ 0 &= \lambda_{e1} S_1 + \lambda_{h1} S_1 + \eta_1 [\lambda_{e1} V_1 + \lambda_{h1} V_1] - Q_1 I_1 \\ 0 &= \alpha_1 \xi_1 I_1 - Q_2 B_1 \\ 0 &= \Lambda_2 - \omega_2 S_2 - \mu_2 S_2 \\ 0 &= \omega_2 S_2 - \mu_2 V_2. \end{aligned} \tag{3.10}$$

From the fourth equation of system (3.10), we get;

$$B_1^* = \frac{\alpha_1 \xi_1 I_1}{Q_2}. \tag{3.11}$$

Substituting equation (3.11) and the limiting values of  $S_1$  and  $V_1$  into the third equation of system (3.10) and solving yields;

$$A I_1^{*3} + B I_1^{*2} + C I_1^* = 0, \tag{3.12}$$

where

$$\begin{aligned} A &= -\alpha_1 \xi_1 \mu_1 \tau_1 Q_1 \\ B &= \phi_1 (\alpha_1^2 \beta_{e1} \Lambda_1 \xi_1 + \alpha_1^2 \beta_{h1} \Lambda_1 \xi_1) - \mu_1 \tau_1 Q_1 (k Q_2 + \alpha_1 \xi_1 m) \\ C &= \phi_1 (\alpha_1^2 \beta_{e1} \Lambda_1 \xi_1 m + \alpha_1 \beta_{h1} \Lambda_1 k Q_2) - k Q_2 m \mu_1 Q_1 \tau_1 \\ \tau_1 &= \mu_1 + \omega_1 \\ \phi_1 &= \mu_1 + \eta_1 \omega_1. \end{aligned}$$

From equation (3.12),  $I_1^* = 0$  is one of the solutions of system (2.1). This corresponds to the disease free equilibrium  $E_0$  and the other solutions when  $I_1^* \neq 0$  gives the relationship between the susceptible, the vaccinated and the infected individuals in the first community. Thus

$$AI_1^{*2} + BI_1^* + C = 0, \tag{3.13}$$

is now considered. The first boundary endemic equilibrium of the system exists if the roots of equation (3.13) are real and positive. Descartes' rule of signs is used to check the possible number of real roots of the polynomial. The number of positive real roots of a polynomial is equal to the number of sign changes in the coefficients of the terms. The coefficients of equation (3.13) are analyzed by first checking the sign of  $A$ . Since all the parameters used are positive, the sign of  $A$  is negative. Next the sign of  $C$  is checked by considering;

$$C = \phi_1(\alpha_1^2 \beta_{e1} \Lambda_1 \xi_1 m + \alpha_1 \beta_{h1} \Lambda_1 k Q_2) - k Q_2 m \mu_1 Q_1 \tau_1$$

which may be expressed as;

$$C = \left[ \frac{\phi_1(\alpha_1^2 \beta_{e1} \Lambda_1 \xi_1 m + \alpha_1 \beta_{h1} \Lambda_1 k Q_2)}{k Q_2 m \mu_1 Q_1 \tau_1} - 1 \right] k Q_2 m \mu_1 Q_1 \tau_1. \tag{3.14}$$

Substituting equation (3.3) into equation (3.14) yields;

$$C = [R_{V1} - 1] k Q_2 m \mu_1 Q_1 \tau_1.$$

Thus  $C > 0$  iff  $R_{V1} > 1$ . Since  $A$  is negative and  $C$  is positive, it implies that there is at least one sign change regardless of the sign of  $B$ . Therefore, equation (3.13) has at least one positive real root. Hence, the first boundary endemic equilibrium point  $E_1$  exists. Similarly, it can be shown that the second boundary endemic equilibrium point ( $E_2$ ), also exists when  $R_{V2} > 1$ .  $\square$

**3.2.6. Local stability of the first boundary endemic steady state ( $E_1$ )**

Cholera is endemic or persistent in the first community if  $S_1^*, V_1^*, I_1^*, B_1^* > 0$  for all  $t > 0$ . The local stability of the first boundary endemic steady state analysis is given in the following theorem,

**Theorem 3.6.** *The first boundary endemic equilibrium of system (2.1) is locally asymptotically stable when  $R_{V1} > 1$ .*

*Proof.* For the first boundary endemic equilibrium point to be stable, then the eigenvalues of it's Jacobian matrix evaluated at  $E_1$ , must have negative real parts. The Jacobian matrix evaluated at  $E_1$  is given by;

$$J(E_1) = \begin{bmatrix} -f_0 & 0 & -f_1 & -f_2 & 0 & 0 \\ \omega_1 & -f_3 & -f_4 & -f_5 & 0 & 0 \\ f_6 & f_7 & f_8 - Q_1 & f_9 & 0 & 0 \\ 0 & 0 & \alpha_1 \xi_1 & -Q_2 & 0 & 0 \\ 0 & 0 & 0 & 0 & -(\mu_2 + \omega_2) & 0 \\ 0 & 0 & 0 & 0 & \omega_2 & -\mu_2 \end{bmatrix},$$

where

$$\begin{aligned} f_0 &= \omega_1 + \mu_1 + \frac{\alpha_1 \beta_{e1} B_1}{k + B_1} + \frac{\alpha_1 \beta_{h1} I_1}{m + I_1} & f_1 &= \frac{\alpha_1 \beta_{h1} \Lambda_1 m}{(\mu_1 + \omega_1)(m + I_1)^2} \\ f_2 &= \frac{\alpha_1 \beta_{e1} \Lambda_1 k}{(\mu_1 + \omega_1)(k + B_1)^2} & f_3 &= \mu_1 + \frac{\eta_1 \alpha_1 \beta_{e1} B_1}{k + B_1} + \frac{\eta_1 \alpha_1 \beta_{h1} I_1}{m + I_1} \\ f_4 &= \frac{\eta_1 \alpha_1 \beta_{h1} \Lambda_1 \omega_1 m}{\mu_1 (\mu_1 + \omega_1)(m + I_1)^2} & f_5 &= \frac{\eta_1 \alpha_1 \beta_{e1} \Lambda_1 \omega_1 k}{\mu_1 (\mu_1 + \omega_1)(k + B_1)^2} \\ f_6 &= \frac{\alpha_1 \beta_{e1} B_1}{k + B_1} + \frac{\alpha_1 \beta_{h1} I_1}{m + I_1} & f_7 &= \frac{\eta_1 \alpha_1 \beta_{e1} B_1}{k + B_1} + \frac{\eta_1 \alpha_1 \beta_{h1} I_1}{m + I_1} \\ f_8 &= \frac{\alpha_1 \beta_{h1} \Lambda_1 m \phi_1}{\mu_1 (\mu_1 + \omega_1)(m + I_1)^2} & f_9 &= \frac{\alpha_1 \beta_{e1} \Lambda_1 \phi_1 k}{\mu_1 (\mu_1 + \omega_1)(k + B_1)^2}. \end{aligned}$$

Clearly, the Jacobian matrix  $J(E_1)$  has two distinct negative eigenvalues given by  $-(\mu_2)$  and  $-(\mu_2 + \omega_2)$ . The local stability is therefore established by computing its other eigenvalues which involves the solution of the system given by;

$$\begin{vmatrix} \lambda + f_0 & 0 & -f_1 & -f_2 \\ \omega_1 & \lambda + f_3 & -f_4 & -f_5 \\ f_6 & f_7 & \lambda - (f_8 + Q_1) & f_9 \\ 0 & 0 & \alpha_1 \xi_1 & \lambda + Q_2 \end{vmatrix} = 0. \tag{3.15}$$

The characteristic equation of equation (3.15) is given by;

$$\lambda^4 + a_0 \lambda^3 + a_1 \lambda^2 + a_2 \lambda + a_3 = 0, \tag{3.16}$$

where

$$a_0 = f_0 + f_3 + Q_1 + Q_2 - f_8$$



$$a_1 = f_0f_3 + f_1f_6 + f_4f_7 + f_0Q_1 + f_3Q_1 + f_0Q_2 + f_3Q_2 + Q_1Q_2 - f_8Q_2 - f_0f_8 - f_3f_8 - \alpha_1\xi_1f_9$$

$$a_2 = f_1f_3f_6 + f_0f_4f_7 - f_0f_3f_8 + f_0f_3Q_1 + f_0f_3Q_2 + f_1f_6Q_2 + f_4f_7Q_2 - f_0f_8Q_2 - f_3f_8Q_2 + f_0Q_1Q_2 + f_3Q_1Q_2 + \alpha_1\xi_1f_2f_6 + \alpha_1\xi_1f_5f_7 - \alpha_1\xi_1f_0f_9 - \alpha_1\xi_1f_3f_9 + \omega_1f_1f_7$$

$$a_3 = f_1f_3f_6Q_2 + f_0f_4f_7Q_2 - f_0f_3f_8Q_2 + f_0f_3Q_1Q_2 + \alpha_1\xi_1f_2f_3f_6 + \alpha_1\xi_1f_0f_5f_7 - \alpha_1\xi_1f_0f_3f_9 + \omega_1f_1f_7Q_2 + \alpha_1\xi_1\omega_1f_2f_7.$$

The number of possible negative zeros of equation (3.16) depends on the signs of  $a_0, a_1, a_2$  and  $a_3$ . This can be analysed using Descartes' Rule of Signs of the polynomial given by;

$$P(\lambda) = a_0\lambda^3 + a_1\lambda^2 + a_2\lambda + a_3 = 0. \tag{3.17}$$

From this Rule, the number of negative real zeros of  $P(\lambda)$  is either equal to the variations in sign of  $P(-\lambda)$  or less than this by an even number. The possibilities of the negative roots of equation (3.17) is as summarized in Table 1.

**Table 3.1:** The Zeros of Characteristic equation (29).

Cases	$a_0$	$a_1$	$a_2$	$a_3$	$R_{V1} > 1$	Sign Change	No. of - Roots
1	+	-	-	+	$R_{V1} > 1$	2	2,0
2	+	-	+	+	$R_{V1} > 1$	2	2,0
3	-	-	+	-	$R_{V1} > 1$	2	2,0
4	+	+	-	-	$R_{V1} > 1$	1	0
5	-	-	+	+	$R_{V1} > 1$	1	0
6	+	+	+	-	$R_{V1} > 1$	1	0
7	-	+	-	+	$R_{V1} > 1$	3	3,1
8	-	-	-	-	$R_{V1} > 1$	0	0

From the table, the maximum number of variations of sign in  $P(-\lambda)$  is three, hence, polynomial (3.17) has three negative roots. Thus,  $J(E_1)$  has five negative real zeros. Therefore, system (2.1) is locally asymptotically stable if  $R_{V2} < 1$ . Clearly, the second boundary endemic steady state is also locally asymptotically stable if  $R_{V1} < 1$ .  $\square$

**3.2.7. Interior endemic equilibrium point**

The model system has a non-trivial equilibrium point in the presence of infection in both communities, known as Interior Endemic equilibrium point given by  $E_3 = (S_1^*, V_1^*, I_1^*, B_1^*, S_2^*, V_2^*, I_2^*, B_2^*) \in \mathbb{R}_+^8$ . This is the point when  $I_i^* > 0$  and  $B_i^* > 0$  for  $i = 1, 2$ , in the two communities.

**Theorem 3.7.** *The interior endemic equilibrium point exists provided  $R_{Vi} > 1$  ( $i = 1, 2$ ).*

*Proof.* At the interior endemic equilibrium point;

$$\begin{aligned}
 0 &< \left(\frac{\alpha_1\beta_{e1}B_1^*}{k+B_1^*} + \frac{\alpha_1\beta_{h1}I_1^*}{m+I_1^*}\right)S_1 + \eta_1\left(\frac{\alpha_1\beta_{e1}B_1^*}{k+B_1^*} + \frac{\alpha_1\beta_{h1}I_1^*}{m+I_1^*}\right)V_1 - Q_1I_1^* \\
 0 &< \alpha_1\xi_1I_1^* - Q_2B_1^* \\
 0 &< \left(\frac{\alpha_2\beta_{e2}B_2^*}{k+B_2^*} + \frac{\alpha_2\beta_{h2}I_2^*}{m+I_2^*}\right)S_2 + \eta_2\left(\frac{\alpha_2\beta_{e2}B_2^*}{k+B_2^*} + \frac{\alpha_2\beta_{h2}I_2^*}{m+I_2^*}\right)V_2 - Q_3I_2^* \\
 0 &< \alpha_2\xi_2I_2^* - Q_4B_2^*.
 \end{aligned} \tag{3.18}$$

From the second and fourth equations of inequality (3.18), we obtain;

$$\begin{aligned}
 B_1^* &< \frac{\alpha_1\xi_1I_1^*}{Q_2} \\
 B_2^* &< \frac{\alpha_2\xi_2I_2^*}{Q_4}.
 \end{aligned}$$

Substituting equation (3.11) and the limiting values of  $S_1$  and  $V_1$  into the second equation of inequality (3.18) and solving for  $I_1^*$  yields equation (3.12) which had been shown to have at least one positive real root in Theorem 3.3. Hence,  $I_1^* > 0$  when  $R_{V1} > 1$ . It is also clear that  $I_2^* > 0$  when  $R_{V2} > 1$ . These imply that  $B_1^* > 0$  and  $B_2^* > 0$ . Therefore the interior endemic equilibrium point ( $E_3$ ) exists when  $R_{V1} > 1$  and  $R_{V2} > 1$ .  $\square$

**3.2.8. Local stability of the interior endemic steady state**

The local stability of the interior endemic equilibrium point is given in the following theorem,

**Theorem 3.8.** *The interior endemic equilibrium of system (2.1) is locally asymptotically stable when  $R_{Vi} > 1$  ( $i = 1, 2$ ).*

*Proof.* To investigate the local stability of the interior endemic equilibrium point ( $E_3$ ), the model system (2.1) is linearized at  $E_3$ . The Jacobian matrix at  $E_3$  is given by;

$$J(E_3) = \begin{bmatrix} -f_0 & 0 & -f_1 & -f_2 & 0 & 0 & 0 & 0 \\ \omega_1 & -f_3 & -f_4 & -f_5 & 0 & 0 & 0 & 0 \\ f_6 & f_7 & f_8 - Q_1 & f_9 & 0 & 0 & a_2 & 0 \\ 0 & 0 & \alpha_1 \xi_1 & -Q_2 & 0 & 0 & 0 & 0 \\ 0 & 0 & 0 & 0 & -g_0 & 0 & -g_1 & -g_2 \\ 0 & 0 & 0 & 0 & \omega_2 & -g_3 & -g_4 & -g_5 \\ 0 & 0 & a_1 & 0 & g_6 & g_7 & g_8 - Q_3 & f_9 \\ 0 & 0 & 0 & 0 & 0 & 0 & \alpha_2 \xi_2 & -Q_4 \end{bmatrix},$$

where

$$\begin{aligned} g_0 &= \omega_2 + \mu_2 + \frac{\alpha_2 \beta_{e2} B_2}{k + B_2} + \frac{\alpha_2 \beta_{h2} I_2}{m + I_2} & g_1 &= \frac{\alpha_2 \beta_{h2} \Lambda_2 m}{(\mu_2 + \omega_2)(m + I_2)^2} \\ g_2 &= \frac{\alpha_2 \beta_{e2} \Lambda_2 k}{(\mu_2 + \omega_2)(k + B_2)^2} & g_3 &= \mu_2 + \frac{\eta_2 \alpha_2 \beta_{e2} B_2}{k + B_2} + \frac{\eta_2 \alpha_2 \beta_{h2} I_2}{m + I_2} \\ g_4 &= \frac{\eta_2 \alpha_2 \beta_{h2} \Lambda_2 \omega_2 m}{\mu_2 (\mu_2 + \omega_2)(m + I_2)^2} & g_5 &= \frac{\eta_2 \alpha_2 \beta_{e2} \Lambda_2 \omega_2 k}{\mu_2 (\mu_2 + \omega_2)(k + B_2)^2} \\ g_6 &= \frac{\alpha_2 \beta_{e2} B_2}{k + B_2} + \frac{\alpha_2 \beta_{h1} I_2}{m + I_2} & g_7 &= \frac{\eta_2 \alpha_2 \beta_{e2} B_2}{k + B_2} + \frac{\eta_2 \alpha_2 \beta_{h2} I_2}{m + I_2} \\ g_8 &= \frac{\alpha_2 \beta_{h2} \Lambda_2 m \phi_2}{\mu_2 (\mu_2 + \omega_2)(m + I_2^*)^2} & g_9 &= \frac{\alpha_2 \beta_{e2} \Lambda_2 \phi_2 k}{\mu_2 (\mu_2 + \omega_2)(k + B_2)^2}. \end{aligned}$$

The Jacobian matrix  $J(E_3)$  can be re-written in the form;

$$J(E_3) = \begin{bmatrix} J_{11} & J_{12} \\ J_{21} & J_{22} \end{bmatrix},$$

where;

$$J_{11} = \begin{bmatrix} -f_0 & 0 & -f_1 & -f_2 \\ \omega_1 & -f_3 & -f_4 & -f_5 \\ f_6 & f_7 & f_8 - Q_1 & f_9 \\ 0 & 0 & \alpha_1 \xi_1 & -Q_2 \end{bmatrix}$$

and

$$J_{22} = \begin{bmatrix} -g_0 & 0 & -g_1 & -g_2 \\ \omega_2 & -g_3 & -g_4 & -g_5 \\ g_6 & g_7 & g_8 - Q_3 & g_9 \\ 0 & 0 & \alpha_2 \xi_2 & -Q_4 \end{bmatrix}.$$

It's clear that  $J_{11}$  and  $J_{22}$  have negative real roots hence,  $J(E_3)$  has negative real zeros and the interior endemic equilibrium point ( $E_3$ ) is locally asymptotically stable.  $\square$

### 4. Numerical Simulations

Numerical Simulations to validate the analytical findings and illustrate the long term dynamics of system (2.1) have been performed using MATLAB. This has been achieved by using parameter values which have been selected from some published literatures as shown in Table 4.1. The parameter values in Table 4.1 give  $R_{V1} = 0.422452 < 1$  and  $R_{V2} = 0.240175 < 1$ . The results of the simulations are presented in the figures below where  $I(t)$  and  $B(t)$  are the number of infected individuals and the concentration of *Vibrio cholerae* in aquatic reservoirs in the two communities at time t respectively.

When  $R_V < 1$ , all the trajectories of the infected population and the concentration of *Vibrios* converge to zero regardless of the presence of intervention strategies as shown in Figure 4.1 and Figure 4.2. This pinpoints that the cholera free state can only be asymptotically stable in line with Theorem 3.3. It also shows that the epidemic size is greatly reduced when vaccination and media awareness are simultaneously deployed.

Figure 4.3 shows that both vaccination and media awareness lower the spread of cholera with time, and that each has an inverse relationship with the spread of the disease. Therefore the rates of vaccination and media awareness should be heightened in order to reduce the outbreak size and duration. Evidently, the effect of media awareness is higher in the control of cholera and it's notable that they should be applied from the start of an outbreak in order to pare the transmission of cholera in any population.

It is also evident from Figure 4.4 that vaccination and media awareness lowers the disease spread, with the first community experiencing earlier disease extinction. This clearly illustrates that the effects of the intervention strategies are unidentical in the two communities and that movement across the communities will lead to re-introduction of the disease in the community where it had been eradicated.

Figure 4.5 shows that migration affects the rate of change of the infected population since, when the rate of movement into the first/second community is higher than the movement out, then the rate of change of the infected individuals increases and vice versa. This attests the fact that migration is a vital factor in the transmission of cholera and hence, movement across cholera hit communities should be circumvented.

**Table 4.1:** Model Parameters and Values.

Parameter	Symbol	Value	Source
Recruitment rate into community $i$	$\Lambda_i$	$9.6274 \times 10^{-5}$ (/day)	[9]
Vaccination rate in community $i$	$\omega_i$	0.78 (/day)	Varies
Vaccine efficacy in community $i$	$\sigma_i$	0.68 (/day)	Estimate
<i>Vibrios</i> ingestion rate in community 1	$\beta_{e1}$	0.075 (/day)	[26]
<i>Vibrios</i> ingestion rate in community 2	$\beta_{e2}$	0.01694 (/day)	[29]
Rate of contact with infectives in com. 1	$\beta_{h1}$	0.0005 (/day)	[25]
Rate of contact with infectives in com. 2	$\beta_{h2}$	0.00125 (/day)	Estimate
Efficacy of media awareness in com. $i$	$\rho_i$	0.75	Varies
Half saturation constant of the pathogen	$k$	$10^6$ cells/l	Estimate
Minimum contact rate with the infected	$m$	0.00001	aries
Natural death rate in community 1	$\mu_1$	0.02 (/day)	[22],[28]
Natural death rate in community 2	$\mu_2$	$5.48 \times 10^{-5}$ (/day)	[27]
Rate of recovery in community 1	$\gamma_1$	0.015 (/day)	[24]
Rate of recovery in community 2	$\gamma_2$	0.2 (/day)	[29]
Disease induced mortality rate in com. 1	$\delta_1$	0.013 (/day)	[23]
Disease induced mortality rate in com. 2	$\delta_2$	$4.0 \times 10^{-4}$ (/day)	[9]
Rate of shedding of <i>Vibrios</i> in com. $i$	$\xi_i$	50 (/day)	[10]
Decay rate of pathogen in com. $i$	$\mu_{ip}$	1.06 (/day)	[10],[27]
Multiplication rate of <i>Vibrios</i> in com. $i$	$g_i$	0.73 (/day)	[10],[27]

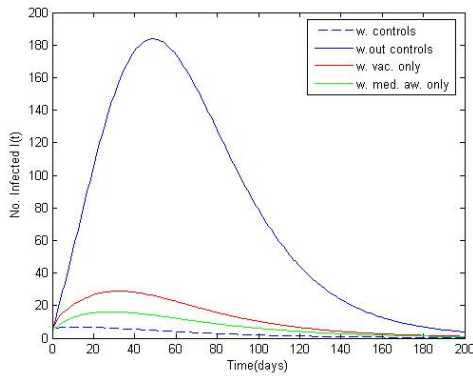


**Figure 4.1:** The number of infectives.

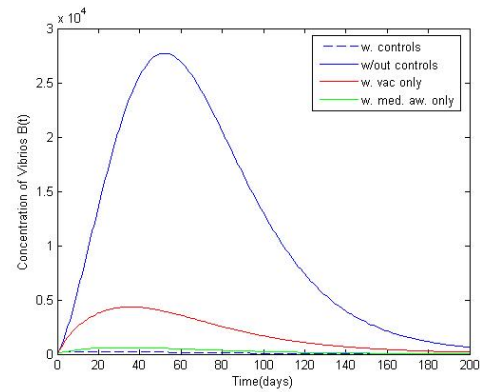


**Figure 4.2:** The concentration of *Vibrios*.

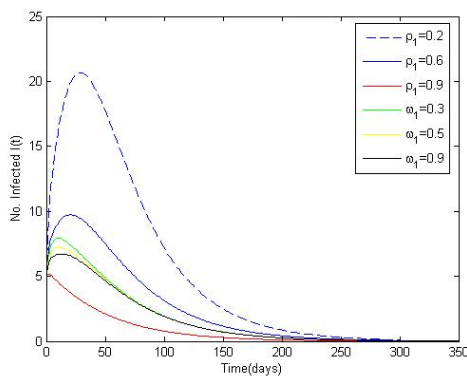


**Figure 4.3:** The number of infectives when varying  $\rho$  and  $\omega$ .

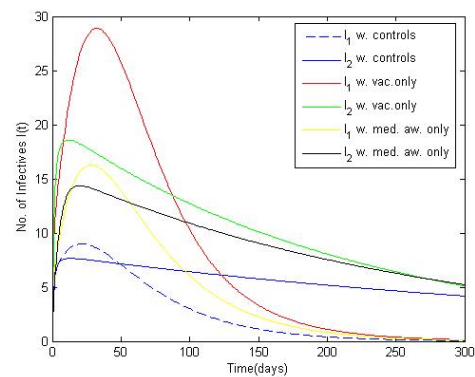


**Figure 4.4:** The number of infectives with and without controls in the two communities.

### 5. Conclusion

A metapopulation model for cholera with imperfect vaccine and variable media awareness was developed and analysed to investigate the long term transmission dynamics of cholera, in the presence of these control strategies. The analytical results of the model indicated that there is a region where the model is mathematically and epidemiologically well posed since its solutions were positive and bounded. The vaccine reproduction numbers for the two isolated communities were computed using the next generation matrix approach. It was also shown that there was no disease transmission when the reproduction numbers were below unity. Stability analysis of the model exhibited that the disease free equilibrium is both locally and globally asymptotically stable when  $R_{Vi} < 1$  ( $i = 1, 2$ ). The model was shown to have four endemic equilibria which were shown to be locally asymptotically stable when  $R_{Vi} > 1$ .

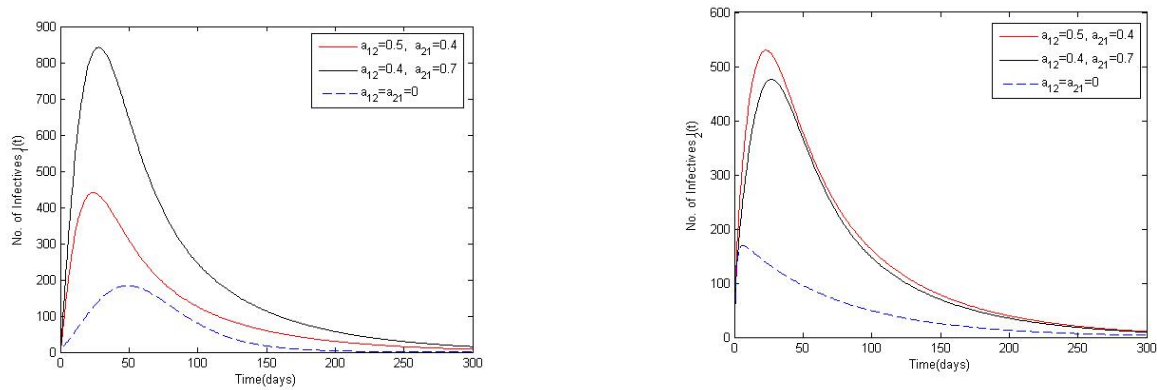


**Figure 4.5:** The rate of change of the infectives when varying the migration parameters.

From the numerical simulations, it was evident that migration of the infected individuals across communities during epidemics, greatly increased the spread of cholera in the two communities. Evidently, effective media awareness and vaccination have also been shown to lower the disease spread resulting into a faster elimination of cholera in the two communities with the first community experiencing earlier disease extinction. This asserts that, the effects of the intervention strategies are unidentical in the two communities and that even with imperfect vaccine, the spread of cholera is greatly pared. Since optimal control and cost effectiveness of vaccination and media awareness have not been done, this can be explored as a future work, to determine the intervention strategy with the least cost and highest efficiency.

## Article Information

**Acknowledgements:** The authors would like to express their sincere thanks to the editor and the anonymous reviewers for their helpful comments and suggestions.

**Author's contributions:** All authors contributed equally to the writing of this paper. All authors read and approved the final manuscript.

**Conflict of Interest Disclosure:** No potential conflict of interest was declared by the authors.

**Copyright Statement:** Authors own the copyright of their work published in the journal and their work is published under the CC BY-NC 4.0 license.

**Supporting/Supporting Organizations:** No grants were received from any public, private or non-profit organizations for this research.

**Ethical Approval and Participant Consent:** It is declared that during the preparation process of this study, scientific and ethical principles were followed and all the studies benefited from are stated in the bibliography.

**Plagiarism Statement:** This article was scanned by the plagiarism program. No plagiarism detected.

## References

- [1] WHO, *Cholera Vaccines: WHO position paper - August 2017*, Weekly Epidemiological Record, **92**(34) (2017), 477-500.
- [2] B. Dumitru, A. Fahimeh, J. Juan, J. Amin, *On a new and generalized fractional model for a real cholera outbreak*, Alex. Eng. J., **61**(11) (2022), 9175 - 9186.
- [3] C. Eric, N. Eric, L. Suzanne, Y. Abdul - Aziz, *Mathematical modeling of the influence of cultural practices on cholera infection in Cameroon*, Math. Biosci. Eng., **18**(6) (2021), 8374-8391.
- [4] Cholera Vaccines, *WHO position paper*, Weekly Epidemiological Record, **85**(13) (2010), 117.
- [5] D. Sur et. al., *Efficacy and safety of a modified killed-whole-cell oral cholera vaccine in India: an interim analysis of a cluster-randomised, double-blind, placebo-controlled trial*, Lancet, **374**(9702) (2009), 1694-1702.
- [6] E. Marcelino et. al., *Effectiveness of mass cholera vaccination in Beira, Mozambique*, N. Engl. J. Med., **352**(8) (2005), 757-767.
- [7] Cholera, *V. Cholerae Infection in Africa*, Available at www.cdc.gov
- [8] N. Hellen, O. Emmanuel, L. Livingstone, *Modeling optimal control of cholera disease under the interventions of vaccination, treatment and education awareness*, J. Math. Res., **10**(5) (2018), 137-152.
- [9] B. Musundi, G. Lawi, F. Nyamwala, *Mathematical analysis of a cholera transmission model incorporating media coverage*, Int. J. Pure Appl. Math., **111**(2) (2016), 219 - 231.
- [10] J. Njagarah, F. Nyabadza, *Modelling optimal control of cholera in communities linked by migration*, Comput. Math. Methods Med., (2015), Article ID 898264.
- [11] L. Rachael, N. Miller, S. Elsa, G. Holly, K. Renee, L. Suzanne, *Modeling optimal intervention strategies for cholera*, Bull. Math. Biol., **72** (2010), 2004-2018.
- [12] R. Michael, H. Joseph, C. Marisa, L. Suzanne, *The impact of spatial arrangements on epidemic disease dynamics and intervention strategies*, J. Biol. Dyn., **10**(1) (2016), 222-249.
- [13] P. Amadi, *A Metapopulation Model for Cholera with Variable Media Efficacy and Imperfect Vaccine*, MSc Thesis, Maseno University (2021).
- [14] Z. Xueyong, S. Xiangyun, W. Ming, *Stochastic modeling with optimal control: Dynamical behavior and optimal control of a stochastic mathematical model for cholera*, Chaos, Solutions and Fractals, **156** (2022), 111854.
- [15] M. Mehmet, B. Zafer, K. Tulay, K. Tahir, *Transmission of cholera disease with Laplacian and triangular parameters*, IJMSI, **17**(2) (2022), 289-305.
- [16] P. Prabir, K. Shyamal, C. Joydev, *Dynamical study in fuzzy threshold dynamics of a cholera epidemic model*, Fuzzy Inf. Eng., **9**(3) (2017), 381-401.
- [17] J. Harris, *Cholera: Immunity and prospects in vaccine development*, J. Infect. Dis., **218**(3) (2018), 141-146 .
- [18] C. Codeco, *Endemic and epidemic dynamics of cholera: The role of the aquatic reservoir*, BMC Infect. Dis., **1**(1) (2001). DOI:10.1186/1471-2334-1-1.
- [19] P. Driessche, W. James, *Reproduction numbers and sub-threshold endemic equilibria for compartmental models of disease transmission*, Math. Biosci., **180** (2002), 29-48.

- [20] C. Leopard, K. Damian, A. Emmanuel, *Modeling and stability analysis for measles metapopulation model with vaccination*, Appl. Comput. Math., **4**(6) (2015), 431-444.
- [21] C. Castillo-Chavez, Z. Feng, W. Huang, *On the computation of  $R_0$  and its role on global stability*, Mathematical Approaches for Emerging and Reemerging Infectious Diseases, **125** (2002), 229-250.
- [22] J. Njagarah, F. Nyabudza, *A metapopulation model for cholera transmission dynamics between communities linked by migration*, Appl. Math. Comput., **241** (2014), 317 - 331.
- [23] C. Jing'an, W. Zhanmin, Z. Xueyong, *Mathematical analysis of a cholera model with vaccination*, J. Appl. Math, **2014**, Article ID 324767, 16 pages.
- [24] M. Jennifer, N. Farai, M. Josiah, *Modelling cholera transmission dynamics in the presence of limited resources*, BMC Res. Notes, **12**(475) (2019).
- [25] H. Nyaberi, D. Malonza, *Mathematical model of cholera transmission with education campaign and treatment through quarantine*, J. Adv. Math. Comput., **32**(3) (2019), 1-12.
- [26] J. Wang, M. Charairat, *Modeling cholera dynamics with controls*, Can. Appl. Math. Q., **19**(3) (2011).
- [27] M. Al-Arydah, A. Mwasu, J. Tchuenche, *Modelling cholera disease with education and chlorination*, J. Biol. Syst., **21**(4) (2013), Article number 1340007.
- [28] M. Yanli, L. Jia-Bao, L. Haixia, *Global dynamics of an SIQR model with vaccination and elimination hybrid strategies*, Mathematics, **6**(12), (2018), 328.
- [29] P. Ana, J. Cristiana, F. Delfim, *A cholera mathematical model with vaccination and the biggest outbreak of world's history*, AIMS Mathematics, **3**(4)(2018), 448 - 463.